

# Street TryOn: Learning In-the-Wild Virtual Try-On from Unpaired Person Images

Aiyu Cui Jay Mahajan Viraj Shah Preeti Gomathinayagam Chang Liu Svetlana Lazebnik  
University of Illinois Urbana-Champaign

<https://cuiaiyu.github.io/StreetTryOn>

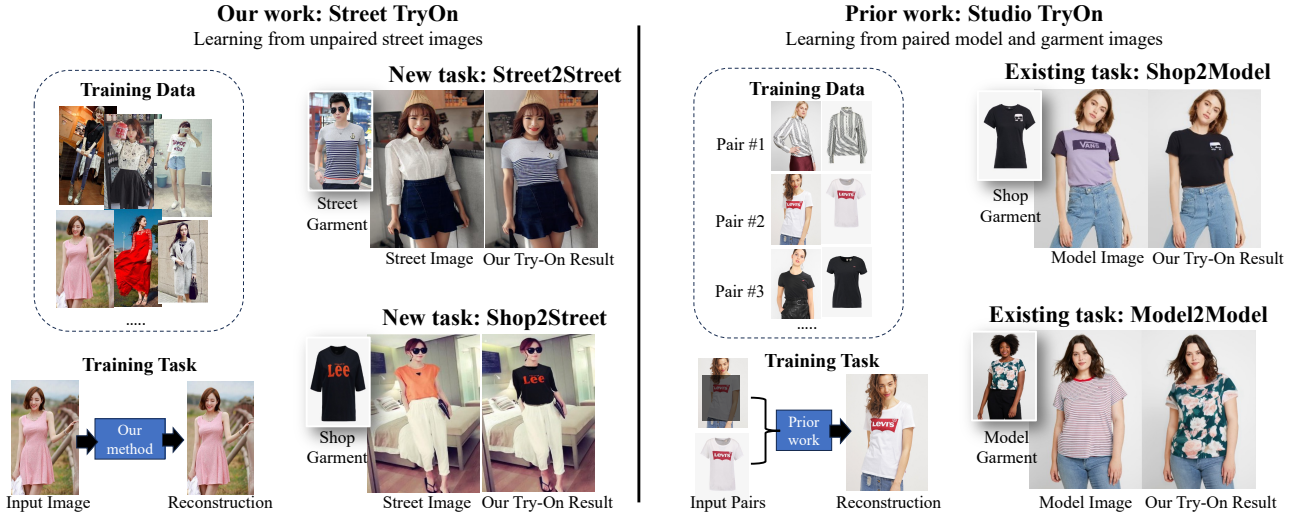


Figure 1. Our proposed Street TryOn benchmark and method, contrasted with existing work focusing on controlled studio images and paired training (see text).

## Abstract

Most existing methods for virtual try-on focus on studio person images with a limited range of poses and clean backgrounds. They can achieve plausible results for this studio try-on setting by learning to warp a garment image to fit a person’s body from paired training data, i.e., garment images paired with images of people wearing the same garment. Such data is often collected from commercial websites, where each garment is demonstrated both by itself and on several models. By contrast, it is hard to collect paired data for in-the-wild scenes, and therefore, virtual try-on for casual images of people with more diverse poses against cluttered backgrounds is rarely studied.

In this work, we fill the gap by introducing a *StreetTryOn* benchmark to evaluate in-the-wild virtual try-on performance and proposing a novel method that can learn it without paired data, from a set of in-the-wild person images directly. Our method achieves robust performance across shop and street domains using a novel DensePose warping correction method combined with diffusion-based conditional inpainting. Our experiments show competitive performance for standard studio try-on tasks and SOTA performance for street try-on and cross-domain try-on tasks.

## 1. Introduction

Virtual try-on methods have advanced rapidly in recent years, reaching high levels of performance for transferring garments from shop images to model person images [12, 17, 35, 39] or from one model image to another [1, 4, 33, 34]. By contrast, transferring garments to and from in-the-wild images is rarely studied. Although the dominant Shop2Model benchmark, VITON-HD [3], is getting saturated, virtual try-on research is still far from robust enough to enable the general population to visualize how a garment would look on their own bodies by taking photos in a casual environment.

Existing virtual try-on methods [1, 4, 12, 17, 33–35, 39] are typically designed for studio images (as shown on the right of Fig. 1) where the models demonstrate garments with a limited range of poses against clean backgrounds and neutral lighting. What is more, these methods train on pairs of images showing the same garment in a shop view and worn by a model, or less frequently, worn by a model in two different poses. Such paired training data makes it possible to directly learn a garment warping module using a reconstruction loss. While this can produce high-quality results in

the studio setting, the resulting methods do not transfer well to more realistic in-the-wild “street” images (Fig. 1, left), in which body poses and camera angles are less constrained, and lighting and backgrounds are more variable. As we will demonstrate, existing methods struggle with limb reconstruction, warping, and background rendering in such images.

Since there is no existing dataset to evaluate virtual try-on in the wild, we introduce a new benchmark, **Street-TryOn**, derived from the large fashion retrieval dataset DeepFashion2 [11] by filtering out over the images that are infeasible for try-on tasks (e.g., non-frontal view, large occlusion, dark environment, etc.), resulting in a set of 12K training and 2K test images. Combining with the garment and person images in VITON-HD [3], we obtain a suite of try-on tasks that have garment and person inputs from various sources. Of primary interest to us are the new tasks of Shop2Street and Street2Street garment transfer (Fig. 1, left), but for completeness, we also include the more traditional tasks of Shop2Model and Model2Model (Fig. 1, right). Benchmarking methods across all these tasks can give a comprehensive idea of the robustness and cross-domain generalization ability of different models (i.e., generalization of models trained on “studio” images to “street” images, and vice versa).

To obtain robust performance on the challenging Shop2Street and Street2Street tasks, we introduce in Section 3 a novel approach for learning virtual try-on from unpaired in-the-wild person images. An overview of our method is shown in Fig. 2. Because the amount of Street-TryOn data is insufficient for training a high-quality model from scratch, we leverage several powerful and robust pre-trained components, most notably, DensePose [13] correspondence to perform garment warping, and diffusion model inpainting to remove the old garment, inpaint skin, and composite the warped target garment onto the person. These components are directly dictated by the challenge of learning from unpaired street images. Without paired training data, it is not possible to directly learn a 2D warping function from source to target images. Instead, DensePose allows us to obtain a warp estimate by registration to a common 3D model. Our warping correction module refines this estimate, with novel training-time data augmentation to mimic registration errors (Section 3.2). Our skin inpainting module addresses the limb reconstruction challenge by leveraging the pre-trained strong diffusion inpainter.

Comprehensive evaluation in Section 4 will show that our method outperforms all existing methods on our Street-TryOn benchmark and is competitive on the much more mature VITON-HD benchmark [3]. Our method is remarkably robust for the hardest try-on setting, Street2Street, achieving similar results whether trained on in-domain or out-of-domain data.

## 2. Related Work

**Virtual Try-On Benchmarks.** Existing Shop2Model virtual try-on benchmarks include VITON [15], VITON-HD [3], MPV [6], and DressCode [27], all of which have paired person and garment images with studio model as person source and ghost mannequin images as garment source. VITON, VITON-HD, and MPV only have top garments, but DressCode also includes other categories like pants and dresses. MPV has more than one person image paired with the garment ghost mannequin images in different poses. DeepFashion[25], and UPT [34] datasets have also been used to demonstrate Model2Model try-on. However, none of the existing datasets are representative of in-the-wild try-on settings. Therefore, our proposed StreetTryOn benchmark is a necessary addition to the literature. The SHHQ-1.0 dataset [10] has previously been proposed to evaluate in-the-wild try-on performance. However, at least 25% images in SHHQ-1.0 are studio model images aggregated from the DeepFashion dataset [25] and the African fashion dataset[14].

**Virtual Try-On Approaches.** Most of the top-performing methods for the Shop2Model try-on [12, 16, 17, 35, 39] are trained on paired datasets mentioned above, like VITON-HD [3] and DressCode [27]. Such methods can achieve high-quality results on in-domain images, but do not transfer well to in-the-wild data. Several other works [1, 4, 39] can achieve Model2Model try-on by training on paired data (people wearing the same outfits in multiple poses). However, such methods cannot be trained in settings where paired data is unavailable. PASTAGAN [33] and PASTAGAN++ [34] are the only prior works for Model2Model try-on trained without paired training data on the UPT dataset [33]. However, our experiments will show that PASTAGAN++ cannot handle the complex backgrounds of street images. Dressing-in-the-wild [7] is another method aimed at in-the-wild try-on, but both its training and inference require videos to learn the person representation.

To capture the complicated appearance distribution of dressed people, a few prior works [23, 26] have used a StyleGAN-like architecture [20] with encoded garments as style codes, but such codes typically have a hard time preserving garment details. PASTAGAN++ [34], one of the few previous methods that can be trained from unpaired data, introduces a sophisticated patch-based garment representation to effectively preserve details. However, its StyleGAN nature makes it fundamentally difficult to train on street images with varied backgrounds.

Learning an explicit flow field for warping from paired data is also popular. Clothflow [16] uses a pyramid architecture to predict flow fields. PFAFN [12] learns flow from the correlation between garment and person; FS-VTON [17] leverages StyleGAN to predict flow; GP-VTON [35] warps garments part by part with multiple local flows. TryOn-

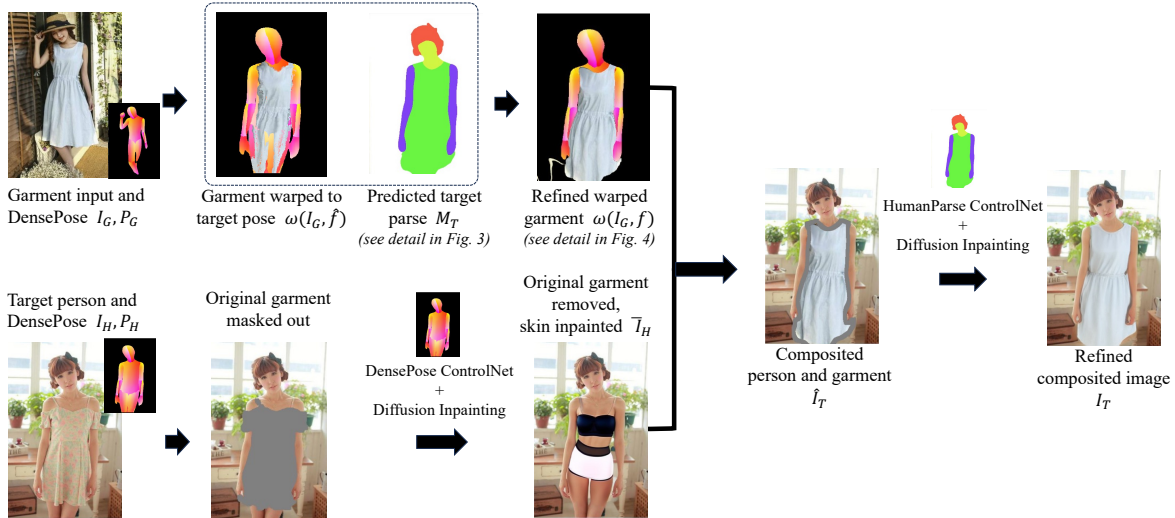


Figure 2. Overview of our proposed virtual try-on method (see text for details).

Diffusion [39] learns implicit flows via cross-attention from paired data. Like our approach, Pose-with-style [1] also uses DensePose to perform warping, but it has to learn from paired data to refine the warping and rendering.

**Diffusion Models** [29–31] have shown a seemingly magical power of image generation. In particular, one can arbitrarily change people’s outfits using text-guided diffusion inpainting. However, this does not provide sufficient control for the virtual try-on task, which requires faithful transfer of a specific garment from another image. To our knowledge, TryOnDiffusion [39] is a specialized diffusion model for virtual try-on so far, trained from scratch on a proprietary dataset of millions of model image pairs. This work has not been released, so we cannot compare with it. By contrast, our method leverages the power of pre-trained diffusion inpainting and only requires the training of a few lightweight additional components, which can be done on a relatively small amount of unpaired data. StableVITON [21] is also a specialized diffusion model that warps garments implicitly using cross-attention in the U-Net, which has to be learned from paired training data. Although StableVITON shows SOTA performance on Shop2Model try-on and promising results for street try-on, it still struggles with garment detail preservation, limb reconstruction, and background rendering. Plus, StableVITON only supports taking garments from the ghost mannequin images, while our methods can allow garments from either shop images or from a person.

Several pretrained diffusion models for text-to-image generation have been released in the past year [29–31]. Stable Diffusion [30] is one of the most accessible because of its open-source code and model weights. It supports inpainting, where one can mask a certain area in an image and fill it in guided by a text prompt. ControlNet [37] enables

tighter conditioning of pre-trained diffusion models using additional inputs like pose and semantic segmentation. We train two DensePose-conditioned ControlNets to enable the removal of the old garment and compositing of the new garment warped to the target pose.

## 2.1. StreetTryOn Benchmark

To explore in-the-wild and cross-domain try-on, we introduce a new benchmark called **StreetTryOn**, derived from the existing fashion retrieval dataset DeepFashion2 [11]. DeepFashion2 contains 191,961 training and 32,153 test images of people with diverse garments and backgrounds, but unfortunately, most of them cannot directly be used for virtual try-on since they only show portions of the body, have large occlusions, non-frontal views, or dark lighting conditions. To remove such unsuitable images, we apply a multi-step filtering process using a combination of provided DeepFashion2 annotations, person detection, and manual selection, resulting in a clean set of 12,364 training and 2,089 test images. More details about the filtering are provided in the supplementary materials.

**Benchmark Tasks.** The try-on tasks of greatest interest to us are **Street2Street**, **Shop2Street**, and **Model2Street** (Fig. 1). For the latter two cross-domain tasks, we obtain the needed shop and model test images from VITON-HD [3]. For **Street2Street**, we use the 2,089 test street images in StreetTryOn, which are partitioned into two subsets of 909 “top” images and 1,190 “dresses.” Then we construct 909 and 1,190 unpaired (person, garment) test tuples by random shuffling. For **Shop2Street** and **Model2Street** try-on, we randomly sample 909 garment ghost mannequin images and 909 model images from VITON-HD to construct two sets of 909 cross-domain (person, garment) test tuples. Com-

binning the above test sets with existing **Shop2Model** and **Model2Model** test sets from VITON-HD gives us a comprehensive suite of scenarios for evaluation.

### 3. Our Try-On Method

An overview of our method is shown in Fig. 2. Given a person image  $I_H$  and a garment image  $I_G$ <sup>1</sup>, our goal is to generate the try-on image  $I_T$  with person  $I_H$  wearing  $I_G$ . We preprocess  $I_H$  and  $I_G$  to obtain human parses  $M_H$  and  $M_G$ , as well as DensePose [13] estimates  $P_H$  and  $P_G$ .

Our try-on inference pipeline starts by predicting the semantic parse  $M_T$  for the try-on output image using a **TryOn Parse Estimator** (Section 3.1). Next, we predict a flow field  $f$  to warp the garment  $I_G$  to the output pose  $P_H$  using DensePose correspondence followed by a trained **Warping Correction Module** (Section 3.2). At the same time, for the person image  $I_H$ , we remove the original garment and inpaint skin regions by a pre-trained diffusion inpainter with a **DensePose ControlNet** conditioned on  $P_H$  (Section 3.3). Then, we combine the warped garment  $\omega(I_G, f)$  and the inpainted person  $\bar{I}_H$  to get the composited person  $I'_T$ . Finally, we use the pre-trained diffusion inpainter with a **Human Parser ControlNet** conditioned on  $M_T$  to inpaint a masked garment boundary to get the final try-on output  $I_T$ .

To summarize, besides the pre-trained DensePose estimator and diffusion inpainter, our method has four learnable components: TryOn Parse Estimator, Warping Correction Module, and the two ControlNets, which are all trained separately without paired data. In the rest of the section, we will describe each of these components in detail.

#### 3.1. TryOn Parse Estimator

Our TryOn Parse Estimator is inspired by ADGAN [26], which uses a pose-guided StyleGAN-like architecture [20] with different style codes encoding person appearance and garments. Although ADGAN’s encodings tend to lose garment details, they work well for capturing garment shapes.

The architecture of our parse estimator is shown in Fig. 3-left. We encode the target DensePose into a  $16 \times 16$  feature map by a trainable encoder, and set it as the initial feature map of the StyleGAN. The style code  $z$  is taken from the input person, with the block corresponding to the try-on garment type replaced by the encoding of the new garment. No noise is injected, and this StyleGAN-based architecture is trained discriminatively.

In more detail, the style code  $z$  is a concatenation of four segment style codes  $\{z^{top}, z^{hair}, z^{pants}, z^{skirt}\}$ . These are the ADGAN segment types with background and skin regions (face, arms, legs) excluded. If we were to encode skin regions, the predicted garment shape, especially sleeve

<sup>1</sup>For simplicity, we use  $I_G$  to denote the garment image with everything except for the try-on garment masked out.

length, would be unduly biased by the shape of the initially visible skin regions. For example, if the original garment of the person has long sleeves, the arm segment will only have hands, which leaks information about the sleeves. Even if the top segment is swapped with a new one with short sleeves, the model will still be biased by the hand segment to predict a long-sleeve garment. Same as in ADGAN, dresses are considered to be the same as tops here.

A segment encoder  $\mathbf{E}_{seg}$  encodes each  $i \in \{top, hair, pants, skirt\}$  as  $z^i = \mathbf{E}(I \odot M^i)$  with the mask  $M_i$  of the segment  $i$  from the human parse  $M$ . At inference time, the top segment will come from the garment image, and the rest will come from the person input, so we predict the human parse as

$$M_T = \mathbf{G}(\{z_G^{top}, z_H^{hair}, z_H^{pants}, z_H^{skirt}\} | \mathbf{E}_{dp}(P_H)) \quad (1)$$

where  $\mathbf{G}$  is the StyleGAN and  $\mathbf{E}_{dp}$  is the DensePose encoder. During training, all segment codes will come from the same person image, and the model is trained to reconstruct the original human parse using cross-entropy loss. We augment the training data by randomly masking the person  $I_H$  with free-form masks [36] to mimic test-time occlusion and applying random shear, scaling, rotation and translation on each extracted segment  $I_H \odot M_H^i$  to teach the model to handle test cases where the garments are not perfectly aligned.

#### 3.2. Warping Correction Module

DensePose is a mapping from a person image to the coordinate system (UV space) of a parametrized 3D human model. In principle, having DensePose estimates for the person and garment image gives us a dense registration between the two, allowing us to transfer garment pixels onto the 3D model and back onto the target human in 2D. However, in practice, there are problems with this approach. DensePose estimates are far from perfect, especially for loose garments, and direct warping also results in many unwrapped areas. Therefore, we follow the DensePose warping step by a trained correction.

As shown in the top of Fig. 3-right, we obtain an initial, or “naive” flow field  $\hat{f}$  by projecting a mesh grid to the UV space using the garment’s DensePose  $P_G$ , and then warping it back to the person’s pose in image space via  $P_H$ . Next, we train a correction module that takes in the naive flow  $\hat{f}$  and gradually adjusts it to obtain the final flow

$$f = \mathbf{C}(\hat{f} | I_G, P_H, M_T). \quad (2)$$

To train the correction module without paired data, we attempt to reconstruct the person image  $I_H$  from a perturbed version  $\bar{I}_H$ . First, we apply a cosine perturbation to the pixel values of DensePose  $P_H$ , which mimics imperfect registration at inference time (see details in the supplementary). Although this changes the the UV coordinates of  $P_H$ ,

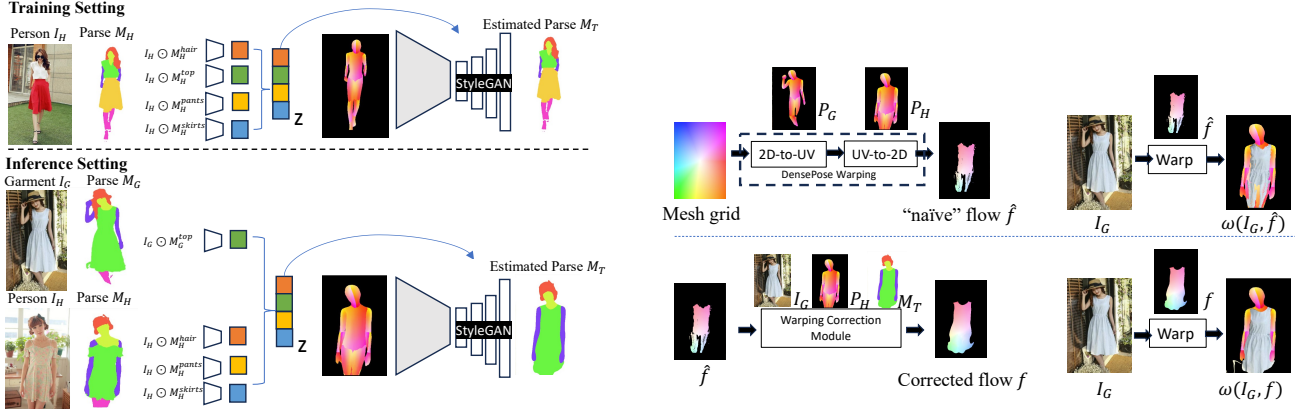


Figure 3. Left: TryOn Parse Estimator (Section 3.1). Right: Warping Correction Module (Section 3.2).

it is still spatially aligned with the original person image  $I_H$ . Next, the cosine-perturbed  $\tilde{P}_H$  and the image  $I_H$  are spatially transformed together using a random affine transformation, translation and rotation to get perturbed versions  $\tilde{P}_H$  and  $\tilde{I}_H$ . Given this synthetic data, we train the corrector  $C$  with the same objectives as in prior work [12, 17]:

$$\begin{aligned} \mathcal{L} = & \mathcal{L}_{smo}(\mathbf{C}(\hat{f}|\tilde{I}_H, P_H, M_H)) \\ & + \|\tilde{I}_H - \omega(\tilde{I}_H, \mathbf{C}(\hat{f}|\tilde{I}_H, P_H, M_H))\| \\ & + \mathcal{L}_{vgg}(\tilde{I}_H, \omega(\tilde{I}_H, \mathbf{C}(\hat{f}|\tilde{I}_H, P_H, M_H))), \end{aligned} \quad (3)$$

where  $\hat{f}$  is the naive flow from  $\tilde{P}_H$  to  $P_H$ ,  $\omega(\cdot, \cdot)$  is a warping operator,  $\mathcal{L}_{smo}$  is total variation loss for smoothing the predicted flow and  $\mathcal{L}_{vgg}$  is L1 loss between VGG features [19].

### 3.3. Inpainting

As explained at the beginning of this section, our pipeline has two inpainting steps: the first is removing the original garment and inpainting skin to get the “undressed” person image  $\tilde{I}_H$ ; the second is refining the composited image  $\hat{I}_T$  to get the final try-on output  $I_T$ .

**Garment Removal and Skin Inpainting.** To prevent information leakage from the mask used to remove the old garment, prior works erase a larger area than necessary (i.e., creating so-called “agnostic” person images [2, 22, 35, 39]) and inpaint the missing skin simultaneously with rendering the warped try-on garment. However, such an approach still struggles with generating limbs in complex poses or removing long or loose sleeves. Moreover, unlike prior works, which only deal with clean backgrounds, we want to preserve as much of the original background as possible. Therefore, before rendering the new garment, we introduce a separate step of removing the original garment and inpainting it with as much skin as possible. To do this by text-guided diffusion inpainting, we use the prompt “a person in a black+ strapless++ bra++++”, where the “+” is used for prompt weighting [8].

**Refining the composited image.** To create the composite

image  $\hat{I}_T$ , we take the predicted try-on garment mask, say  $M_T^{top}$ , out of the predicted parse  $M_T$  and combine it with the “undressed” person image  $\tilde{I}_H$  as

$$\hat{I}_T = \tilde{I}_H \odot e[1 - M_T^{top}] + \omega(I_G, \hat{f}) \odot e[M_T^{top}], \quad (4)$$

where  $e[\cdot]$  is an erosion operator to create a masked region along the garment boundary for the inpainter to refine, since this is the source of many errors and misalignments between the body and the warped garment tend to concentrate. Because the diffusion inpainter also tends to introduce minor changes in the image outside the inpainting mask, we copy and paste the person’s face from the original person image  $I_H$  to avoid distortion.

Both of the above steps are accomplished by a pre-trained Stable Diffusion inpainter [9] combined with ControlNets [37] trained on our own data. Specifically, for skin inpainting, we train a ControlNet using DensePose  $P_H$  as conditioning information, and for the final compositing, we train a ControlNet with predicted parse  $M_T$  as conditioning. Additional implementation details are given in Section 4 and the supplementary material.

## 4. Experiments

### 4.1. StreetTryOn Benchmark

To explore in-the-wild and cross-domain try-on, we introduce a new benchmark called **StreetTryOn**, derived from the existing fashion retrieval dataset DeepFashion2 [11]. DeepFashion2 contains 191,961 training and 32,153 test images of people with diverse garments and backgrounds, but unfortunately, most of them cannot directly be used for virtual try-on since they only show portions of the body, have large occlusions, non-frontal views, or dark lighting conditions. To remove such unsuitable images, we apply a multi-step filtering process using a combination of provided DeepFashion2 annotations, person detection, and manual selection, resulting in a clean set of 12,364 training and 2,089 test images. More details about the filtering are provided in the supplementary materials.

**Benchmark Tasks.** The try-on tasks of greatest interest to us are **Street2Street**, **Shop2Street**, and **Model2Street** (Fig. 1). For the latter two cross-domain tasks, we obtain the needed shop and model test images from VITON-HD [3]. For **Street2Street**, we use the 2,089 test street images in StreetTryOn, which are partitioned into two subsets of 909 “top” images and 1,190 “dresses.” Then we construct 909 and 1,190 unpaired (person, garment) test tuples by random shuffling. For **Shop2Street** and **Model2Street** try-on, we randomly sample 909 garment ghost mannequin images and 909 model images from VITON-HD to construct two sets of 909 cross-domain (person, garment) test tuples. Combining the above test sets with existing **Shop2Model** and **Model2Model** test sets from VITON-HD gives us a comprehensive suite of scenarios for evaluation.

## 4.2. Implementation Details

**Evaluation Metrics.** For all tests, we evaluate performance with the standard FID metric [18], which measures the similarity of the output data distribution with the target data. Additionally, we report SSIM [32] and LPIPS [38] for image reconstruction quality when paired test tuples are available. We run experiments at  $512 \times 320$  resolution when the target person is from StreetTryOn (Shop2Street, Model2Street, and Street2Street tests) and  $512 \times 384$  resolution when the target person is from VITON-HD (Shop2Model and Model2Model).

**Implementation Details.** We obtain human DensePose using the method of Guler et al. [13], garment DensePose using the method of Cui et al. [5], and human parse (semantic segmentation) using SCHP [24]. Our TryOn Parse Estimator is trained with a learning rate  $1e - 4$  and batch size 8 for 100 epochs. Our Warping Correction module has the same architecture as the one in Clothflow [16]; however, unlike Clothflow, which predicts a warping flow from scratch, we start with the DensePose-warped flow and gradually correct it. We train our model with a learning rate of  $1e - 5$  for 100 epochs. For inpainting, we use the Stable Diffusion inpainter from the diffusers library [28] and train DensePose and Human Parse ControlNets in the default setting with an empty prompt for 50 epochs.

## 4.3. Comparative Evaluation

Next, we present our main experimental results. To evaluate the power of unpaired training on in-the-wild data, we compare three training settings for our method: (1) training with the standard paired VITON-HD training data; (2) unpaired training with VITON-HD person images only; (3) unpaired training with Street TryOn person images.

### 4.3.1 Garment Transfer from Person Images.

Tab. 1 reports results for in-the-wild try-on task Street2Street, cross-domain task Model2Street, and studio task Model2Model. All of these take garments from person images (either studio or street). For all these settings, it is interesting to see that the training regime makes little difference for our method. This validates the robustness of all the major components of our method: TryOn Parse Estimator, DensePose warping, and ControlNet Inpainting. Fig. 4 shows qualitative examples of our Street2Street results, further confirming its strong performance across poses, garment styles, and cluttered backgrounds.

In Tab. 1, we compare performance with Shop2Model methods FS-VTON, SDAFN and HR-VTON, which we retrain for Model2Model try-on using the DeepFashion dataset [25]. We also compare with Pose-with-Style (PWS) and PASTAGAN++, both of which are StyleGANs with customized warping designs trained in a model-to-model setting with clean backgrounds. In addition, we train PASTAGAN++ from scratch with the street images in the proposed Street TryOn benchmark, reported as PASTAGAN++ (street). In terms of FID, these methods do much worse than ours on street images, and Fig. 5 shows why: they frequently produce warping artifacts and cannot cope with complex backgrounds. One might wonder whether the higher FIDs of competing methods are primarily due to their failure to render the background. However, in Section 4.4 (Fig. 6), we will present an ablation study demonstrating that even if the background is not taken into account, our method still achieves the best performance.

	Street2Street FID ↓	Model2Street FID ↓	Model2Model FID ↓
Ours (Paired, VITON-HD)	33.165	<b>34.050</b>	10.961
Ours (Unpaired, VITON-HD)	33.742	34.434	11.040
Ours (Unpaired, StreetTryOn)	<b>33.039</b>	34.191	<b>10.214</b>
FS-VTON [17]	67.009	77.273	13.926
HR-VTON [22]	63.539	55.172	20.404
SDAFN [2]	42.432	44.537	14.316
PWS [1]	84.326	76.889	34.224
PastaGAN++ [34]	67.016	71.090	13.848
PastaGAN++ (street)	67.088	70.461	40.841

Table 1. **Evaluation on Street2Street, Model2Street, and Model2Model tests.** We retrain FS-VTON, HR-VTON and SD-VTON on paired DeepFashion dataset for Model2Model try-on at  $512 \times 320$ . PWS is trained on paired DeepFashion [25], and PASTAGAN++ is trained on UPT dataset [33]. PASTAGAN++ (street) is trained on the proposed Street TryOn dataset.

### 4.3.2 Garment Transfer from Shop Images.

Tab. 2 presents an evaluation on Shop2Street and Shop2Model tasks, in which a garment from a ghost mannequin image is transferred to a person image. Here, we compare performance to SOTA Shop2Model methods PBAFN [12], FS-VTON [17], SDAFN [2], GP-VTON [35],

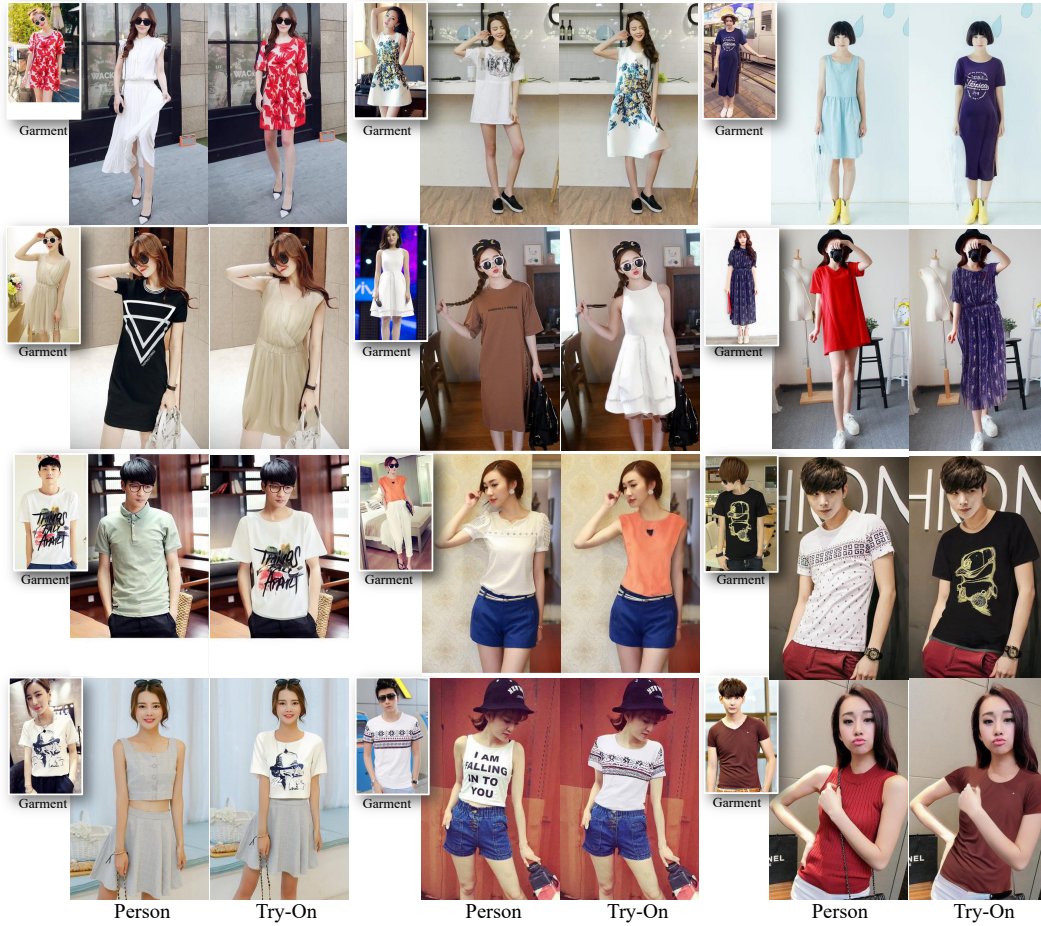


Figure 4. Street2Street Try-On examples for our method.



(a) Comparisons with methods trained on the Model2Model setting

(b) Comparison with methods trained on the Shop2Model setting

Figure 5. (a)-top: Model2Street. (a)-bottom: Model2Model. (b)-top: Shop2Street. (b)-bottom: Shop2Model.

	Shop2Street FID ↓	Shop2Model (VITON-HD) FID ↓ SSIM ↑ LPIPS ↓		
Ours (Paired, VITON-HD)	<b>33.819</b>	9.671	0.840	0.113
Ours (Unpaired, VITON-HD)	35.135	11.675	0.826	0.128
Ours (Unpaired, StreetTryOn)	34.054	11.951	0.823	0.129
SDAFN [2]	62.735	9.400	0.882	0.092
FS-VTON [17]	77.843	9.552	0.883	0.091
HR-VTON [22]	63.516	16.21	0.862	0.109
GP-VTON [35]	n.a.	9.197	0.894	0.080
StableVITON [21]	37.085	<b>8.233</b>	<b>0.888</b>	<b>0.073</b>

Table 2. **Evaluation on Shop2Street and Shop2Model tests** at  $512 \times 320$  and  $512 \times 384$  respectively. The methods are retrained at  $512 \times 384$  if their released models have a lower resolution. We resize output images to the resolution for these methods with released models at higher resolutions.

and StableVITON [21]. Our method gets the best performance on the cross-domain Shop2Street task, confirming both its robustness and the challenging nature of our Street TryOn benchmark. Fig. 5 compares some qualitative results for Shop2Street. For most prior methods, both the warping and rendering steps tend to fail on out-of-domain street images, which is also evident in the concurrent work, StableVITON [21]. Although StableVITON shows significant improvement compared to other prior work on Shop2Street try-on, it still struggles in limb reconstruction and background rendering (Example 1 in Fig.5, right) because its agnostic person inputs tend to erase too much skin/background area. Instead, our proposed garment-removal and skin-inpainting module can better reconstruct the in-the-wild person input. In addition, the garment reconstruction of StableVITON is not as robust as ours, because it is trained on paired studio images, which fail to fully capture the diverse distribution of in-the-wild person images.

The last three columns of Tab. 2 present a comparative evaluation on the Shop2Model (VITON-HD) task. The competing methods, which are highly tuned on VITON-HD paired data, obtain FID, SSIM, and LPIPS scores that are very close together, suggesting that the VITON-HD benchmark is nearing saturation. Our method comes within striking distance, but does not reach quite the same level quantitatively. While we train each component of our method separately, the other works jointly train the warping and refinement modules so they can better learn to complement one another. They also tend to train their flow prediction from scratch on the target dataset instead of relying on off-the-shelf DensePose. Such custom-trained flow modules give more accurate in-domain results but do not generalize well to out-of-dataset test images as we have seen. Additionally, some of these methods [12, 17, 35] include a custom blending mask to eliminate the back of the garment visible in the neck area of the ghost mannequin image. Fig. 5 shows qualitative examples of Shop2Model try-on. While our method sometimes suffers from artifacts, it has its advantages as well: it better preserves the arms, especially for hard poses, or where long sleeves need to be replaced with short ones.

	FG-tryon only (w/o BG)	FG-tryon + BG inpainted	end-to-end (w/ BG)
FS-VTON	35.137	53.018	67.009
HR-VTON	41.154	55.857	63.539
SDAFN	34.274	47.634	42.436
PASTAGAN++	36.267	49.732	67.016
Ours	<b>31.218</b>	<b>46.178</b>	<b>33.039</b>

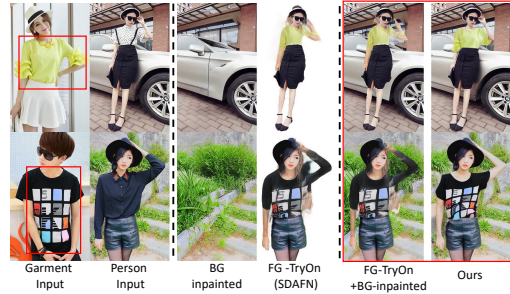


Figure 6. The influence of image background in Street2Street try-on task. We report Street2Street try-on for segmented foreground try-on only (FG-tryon), foreground try-on blended with inpainted background (FG-tryon + BG inpainted), and running inference for each model without foreground segmentation (end-to-end). (Top): Quantitative comparisons with FS-VTON, SDAFN, HR-VTON, and PASTAGAN++, which are all **retrained** for Model2Model try-on, if any is originally not trained for another setting. (Bottom): Visual comparison with the best prior method, SDAFN.

## 4.4. Ablation Study

### 4.4.1 Background rendering is not the only challenge for street try-on.

A reasonable inquiry is whether the main reason that studio-trained methods get bad FID scores on street images is their failure to render the complex background. Fig. 6 presents an ablation study that factors out the effect of the background. To do this, we run Model2Model methods on the segmented foreground person and blend the result with the original background that has the missing area inpainted by Stable Diffusion inpainter. The table in Fig. 6 compares the FID scores for three SOTA Model2Model methods with ours in three settings: foreground only, foreground blended with inpainted background, and end-to-end (inference without foreground segmentation). We can see that even the best prior method (SDAFN retrained on Model2Model) does not do as well as ours. Thus, studio-trained Model2Model methods are insufficient for in-the-wild try-on, especially for limb reconstruction and garment warping.

### 4.4.2 Effectiveness of each component.

Fig. 7 show an ablation study to verify the effectiveness of each component of our method. We start with a baseline (A), in which we directly inpaint the masked-out regions of the person’s original garment with a CLIP [28] image embedding of the new garment. Then we add the following components one by one: (B) DensePose warping, (C) skin





(a) Visual Results.

	Shop2Shop Top	Shop2Street Top	Model2Street Top	Street2Street Dress	Street2Street Top
A	54.482	62.247	59.732	100.587	59.665
B	22.942	36.319	34.412	38.974	34.853
C	14.024	<b>35.368</b>	34.218	<b>34.115</b>	34.009
D	<b>11.951</b>	35.632	<b>34.191</b>	34.741	<b>33.039</b>

(b) Quantitative Results (FID).

Figure 7. Ablation study. (A) Baseline that inpaints the masked-out original garment with CLIP vision embedding of the input garment; (B) adding DensePose warping; (C) adding skin inpainting on top of B; (D) adding warping correction on top of C.

Inpainting, and (D) Warping Correction. The results show that directly generating the garments without warping cannot reconstruct the garment details (Fig. 7 A). Without the proposed skin inpainting, the result will be biased toward the shape of the original garment (Fig. 7 B). Lastly, without the warping correction, we cannot properly reconstruct high-frequency textures like stripes (Fig. 7 C).

Note that in Fig. 7-a, the FID discrepancy is not large between (C) and (D) when the person is from the street. The reason is that the complex backgrounds in the street images reduce the difference in data distributions, so FID does not clearly reflect the improvement in texture refinement. Instead, the effectiveness of the warping correction module can be clearly seen in the Shop2Model test, where the person images have a clean background so that the FID can focus on the garment details.

Finally, we report an ablation study that separately analyzes the effects of our DensePose warping and inpainting-based compositing. We take FS-VTON [17], a non-diffusion-based method with separate warping and refinement modules, whose warping module is trained using paired studio images. We individually replace our warping and refinement modules with theirs. Here, our method is trained with paired data on VITON-HD for a fair comparison. As shown in Fig. 8, both our proposed warping module and the diffusion model significantly improve performance.

## 5. Conclusion

In this work, we have introduced a new **StreetTryOn** benchmark and proposed a try-on method leveraging powerful pre-trained pose estimation and inpainting networks to



Figure 8. Comparison with warping and compositing (fusion) modules of FS-VITON [17] in FID. **Top:** Visual Results. **Bottom:** Quantitative Results.

robustly transfer garments to and from in-the-wild images. Although our method shows promising results, it still has room to improve, as shown by the failure cases in Fig. 9. In particular, our method cannot perform relighting, inherits artifacts like bad hand generation from Stable Diffusion, and does not always preserve garment details. With more fine-tuning and better correction modules, many of these issues can be alleviated.



Figure 9. Failure cases. (Top-left) The camera is treated as part of the shirt. (Bottom-left) Warping failure. (Top-right) Failure to preserve garment details, hand artifact. (Bottom-right) lighting mismatch, neck artifact.

## References

- [1] Badour AlBahar, Jingwan Lu, Jimei Yang, Zhixin Shu, Eli Shechtman, and Jia-Bin Huang. Pose with Style: Detail-Preserving Pose-Guided Image Synthesis with Conditional StyleGAN. *ACM Transactions on Graphics (TOG)*, 40(6): 1–11, 2021. [1](#), [2](#), [3](#), [6](#)
- [2] Shuai Bai, Huiling Zhou, Zhikang Li, Chang Zhou, and Hongxia Yang. Single Stage Virtual Try-on via Deformable Attention Flows. In *European Conference on Computer Vision*, pages 409–425. Springer, 2022. [5](#), [6](#), [8](#), [15](#)
- [3] Seunghwan Choi, Sunghyun Park, Minsoo Lee, and Jaegul Choo. VITON-HD: High-Resolution Virtual Try-On via Misalignment-Aware Normalization. In *Proceedings of the IEEE/CVF Conference on Computer Vision and Pattern Recognition*, pages 14131–14140, 2021. [1](#), [2](#), [3](#), [6](#), [16](#), [17](#)
- [4] Aiyu Cui, Daniel McKee, and Svetlana Lazebnik. Dressing in Order: Recurrent Person Image Generation for Pose Transfer, Virtual Try-on and Outfit Editing. In *Proceedings of the IEEE/CVF international conference on computer vision*, pages 14638–14647, 2021. [1](#), [2](#)
- [5] Aiyu Cui, Sen He, Tao Xiang, and Antoine Toisoul. Learning Garment Densepose for Robust Warping in Virtual Try-On. *arXiv preprint arXiv:2303.17688*, 2023. [6](#), [14](#)
- [6] Haoye Dong, Xiaodan Liang, Xiaohui Shen, Bochao Wang, Hanjiang Lai, Jia Zhu, Zhiting Hu, and Jian Yin. Towards Multi-pose Guided Virtual Try-on Network. In *Proceedings of the IEEE/CVF international conference on computer vision*, pages 9026–9035, 2019. [2](#)
- [7] Xin Dong, Fuwei Zhao, Zhenyu Xie, Xijin Zhang, Daniel K Du, Min Zheng, Xiang Long, Xiaodan Liang, and Jianchao Yang. Dressing in the Wild by Watching Dance Videos. In *Proceedings of the IEEE/CVF Conference on Computer Vision and Pattern Recognition*, pages 3480–3489, 2022. [2](#)
- [8] Hugging Face. Prompt weighting. [https://huggingface.co/docs/diffusers/using-diffusers/weighted\\_prompts](https://huggingface.co/docs/diffusers/using-diffusers/weighted_prompts), . [5](#)
- [9] Hugging Face. Stable diffusion inpainting. <https://huggingface.co/runwayml/stable-diffusion-inpainting>, . [5](#), [14](#)
- [10] Jianglin Fu, Shikai Li, Yuming Jiang, Kwan-Yee Lin, Chen Qian, Chen Change Loy, Wayne Wu, and Ziwei Liu. Stylegan-human: A data-centric odyssey of human generation. In *European Conference on Computer Vision*, pages 1–19. Springer, 2022. [2](#)
- [11] Yuying Ge, Ruimao Zhang, Xiaogang Wang, Xiaoou Tang, and Ping Luo. DeepFashion2: A Versatile Benchmark for Detection, Pose Estimation, Segmentation and Re-Identification of Clothing Images. In *Proceedings of the IEEE/CVF Conference on Computer Vision and Pattern Recognition*, pages 5337–5345, 2019. [2](#), [3](#), [5](#), [12](#)
- [12] Yuying Ge, Yibing Song, Ruimao Zhang, Chongjian Ge, Wei Liu, and Ping Luo. Parser-Free Virtual Try-on via Distilling Appearance Flows. In *Proceedings of the IEEE/CVF Conference on Computer Vision and Pattern Recognition*, pages 8485–8493, 2021. [1](#), [2](#), [5](#), [6](#), [8](#), [15](#)
- [13] Riza Alp Güler, Natalia Neverova, and Iasonas Kokkinos. DensePose: Dense Human Pose Estimation In The Wild. In *Proceedings of the IEEE Conference on Computer Vision and Pattern Recognition*, pages 7297–7306, 2018. [2](#), [4](#), [6](#), [12](#)
- [14] Gilles Hacheme and Nouréini Sayouti. Neural fashion image captioning: Accounting for data diversity. *arXiv preprint arXiv:2106.12154*, 2021. [2](#)
- [15] Xintong Han, Zuxuan Wu, Zhe Wu, Ruichi Yu, and Larry S Davis. VITON: An Image-Based Virtual Try-on Network. In *Proceedings of the IEEE conference on computer vision and pattern recognition*, pages 7543–7552, 2018. [2](#)
- [16] Xintong Han, Xiaojun Hu, Weilin Huang, and Matthew R Scott. ClothFlow: A Flow-Based Model for Clothed Person Generation. In *Proceedings of the IEEE/CVF International Conference on Computer Vision*, pages 10471–10480, 2019. [2](#), [6](#)
- [17] Sen He, Yi-Zhe Song, and Tao Xiang. Style-Based Global Appearance Flow for Virtual Try-On. In *Proceedings of the IEEE/CVF Conference on Computer Vision and Pattern Recognition*, pages 3470–3479, 2022. [1](#), [2](#), [5](#), [6](#), [8](#), [9](#), [15](#)
- [18] Martin Heusel, Hubert Ramsauer, Thomas Unterthiner, Bernhard Nessler, and Sepp Hochreiter. GANs Trained by a Two Time-Scale Update Rule Converge to a Local Nash Equilibrium. *Advances in Neural Information Processing Systems*, 30, 2017. [6](#)
- [19] Justin Johnson, Alexandre Alahi, and Li Fei-Fei. Perceptual Losses for Real-Time Style Transfer and Super-Resolution. In *Computer Vision—ECCV 2016: 14th European Conference, Amsterdam, The Netherlands, October 11–14, 2016, Proceedings, Part II 14*, pages 694–711. Springer, 2016. [5](#)
- [20] Tero Karras, Samuli Laine, and Timo Aila. A Style-Based Generator Architecture for Generative Adversarial Networks. In *Proceedings of the IEEE/CVF Conference on Computer Vision and Pattern Recognition*, pages 4401–4410, 2019. [2](#), [4](#)
- [21] Jeongho Kim, Gyojung Gu, Minho Park, Sunghyun Park, and Jaegul Choo. Stableviton: Learning semantic correspondence with latent diffusion model for virtual try-on. *arXiv preprint arXiv:2312.01725*, 2023. [3](#), [8](#)
- [22] Sangyun Lee, Gyojung Gu, Sunghyun Park, Seunghwan Choi, and Jaegul Choo. High-Resolution Virtual Try-On

- with Misalignment and Occlusion-Handled Conditions. In *European Conference on Computer Vision*, pages 204–219. Springer, 2022. 5, 6, 8
- [23] Kathleen M Lewis, Srivatsan Varadharajan, and Ira Kemelmacher-Shlizerman. TryOnGAN: Body-Aware Try-on via Layered Interpolation. *ACM Transactions on Graphics (TOG)*, 40(4):1–10, 2021. 2
- [24] Peike Li, Yunqiu Xu, Yunchao Wei, and Yi Yang. Self-Correction for Human Parsing. *IEEE Transactions on Pattern Analysis and Machine Intelligence*, 44(6):3260–3271, 2020. 6
- [25] Ziwei Liu, Ping Luo, Shi Qiu, Xiaogang Wang, and Xiaoou Tang. Deepfashion: Powering Robust Clothes Recognition and Retrieval with Rich Annotations. In *Proceedings of the IEEE Conference on Computer Vision and Pattern Recognition*, pages 1096–1104, 2016. 2, 6, 14
- [26] Yifang Men, Yiming Mao, Yuning Jiang, Wei-Ying Ma, and Zhouhui Lian. Controllable Person Image Synthesis with Attribute-Decomposed GAN. In *Proceedings of the IEEE/CVF Conference on Computer Vision and Pattern Recognition*, pages 5084–5093, 2020. 2, 4
- [27] Davide Morelli, Matteo Fincato, Marcella Cornia, Federico Landi, Fabio Cesari, and Rita Cucchiara. Dress Code: High-resolution Multi-Category Virtual Try-On. In *Proceedings of the IEEE/CVF Conference on Computer Vision and Pattern Recognition*, pages 2231–2235, 2022. 2
- [28] Alec Radford, Jong Wook Kim, Chris Hallacy, Aditya Ramesh, Gabriel Goh, Sandhini Agarwal, Girish Sastry, Amanda Askell, Pamela Mishkin, Jack Clark, et al. Learning Transferable Visual Models from Natural Language Supervision. In *International Conference on Machine Learning*, pages 8748–8763. PMLR, 2021. 6, 8
- [29] Aditya Ramesh, Prafulla Dhariwal, Alex Nichol, Casey Chu, and Mark Chen. Hierarchical Text-Conditional Image Generation with CLIP Latents. *arXiv preprint arXiv:2204.06125*, 1(2):3, 2022. 3
- [30] Robin Rombach, Andreas Blattmann, Dominik Lorenz, Patrick Esser, and Björn Ommer. High-resolution image synthesis with latent diffusion models. In *Proceedings of the IEEE/CVF Conference on Computer Vision and Pattern Recognition*, pages 10684–10695, 2022. 3
- [31] Chitwan Saharia, William Chan, Saurabh Saxena, Lala Li, Jay Whang, Emily L Denton, Kamyar Ghasemipour, Raphael Gontijo Lopes, Burcu Karagol Ayan, Tim Salimans, et al. Photorealistic Text-to-Image Diffusion Models with Deep Language Understanding. *Advances in Neural Information Processing Systems*, 35:36479–36494, 2022. 3
- [32] Zhou Wang, Alan C Bovik, Hamid R Sheikh, and Eero P Simoncelli. Image Quality Assessment: From Error Visibility to Structural Similarity. *IEEE Transactions on Image Processing*, 13(4):600–612, 2004. 6
- [33] Zhenyu Xie, Zaiyu Huang, Fuwei Zhao, Haoye Dong, Michael Kampffmeyer, and Xiaodan Liang. Towards scalable unpaired virtual try-on via patch-routed spatially-adaptive gan. *Advances in Neural Information Processing Systems*, 34:2598–2610, 2021. 1, 2, 6
- [34] Zhenyu Xie, Zaiyu Huang, Fuwei Zhao, Haoye Dong, Michael Kampffmeyer, Xin Dong, Feida Zhu, and Xiaodan Liang. Pasta-gan++: A versatile framework for high-resolution unpaired virtual try-on. *arXiv preprint arXiv:2207.13475*, 2022. 1, 2, 6
- [35] Zhenyu Xie, Zaiyu Huang, Xin Dong, Fuwei Zhao, Haoye Dong, Xijin Zhang, Feida Zhu, and Xiaodan Liang. GP-VTON: Towards General Purpose Virtual Try-on via Collaborative Local-Flow Global-Parsing Learning. In *Proceedings of the IEEE/CVF Conference on Computer Vision and Pattern Recognition*, pages 23550–23559, 2023. 1, 2, 5, 6, 8, 15
- [36] Jiahui Yu, Zhe Lin, Jimei Yang, Xiaohui Shen, Xin Lu, and Thomas S Huang. Free-Form Image Inpainting with Gated Convolution. In *Proceedings of the IEEE/CVF International Conference on Computer Vision*, pages 4471–4480, 2019. 4
- [37] Lvmin Zhang, Anyi Rao, and Maneesh Agrawala. Adding Conditional Control to Text-to-Image Diffusion Models. In *Proceedings of the IEEE/CVF International Conference on Computer Vision*, pages 3836–3847, 2023. 3, 5
- [38] Richard Zhang, Phillip Isola, Alexei A Efros, Eli Shechtman, and Oliver Wang. The Unreasonable Effectiveness of Deep Features as a Perceptual Metric. In *CVPR*, 2018. 6
- [39] Luyang Zhu, Dawei Yang, Tyler Zhu, Fitsum Reda, William Chan, Chitwan Saharia, Mohammad Norouzi, and Ira Kemelmacher-Shlizerman. TryOnDiffusion: A Tale of Two UNets. In *Proceedings of the IEEE/CVF Conference on Computer Vision and Pattern Recognition*, pages 4606–4615, 2023. 1, 2, 3, 5

# Appendices

<b>A Street TryOn Benchmark Details</b>	<b>12</b>
A.1. Data Filtering Processes . . . . .	12
A.2. Data Statistics . . . . .	12
<b>B DensePose Perturbation with Cosine Noise</b>	<b>13</b>
<b>C Additional Implementation Details</b>	<b>13</b>
C.1. Pre-trained Diffusion Models . . . . .	13
C.2. Garment DensePose Detection . . . . .	14
<b>D More Visual Results</b>	<b>14</b>
D.1. Shop2Model Test . . . . .	15
D.2. Street2Street Test . . . . .	15
D.3. Ablation Study . . . . .	15

## A. Street TryOn Benchmark Details

The proposed Street TryOn benchmark is derived from the Fashion Retrieval Dataset DeepFashion2 [11]. DeepFashion2 releases 191,961 and 32,153 in-the-wild fashion images for training and validation. These images feature models wearing an assortment of clothing items belonging to 13 popular clothing categories. For each image, a comprehensive set of annotations is available, encompassing information on scale, occlusion, zoom-in level, viewpoint, category, style, bounding box coordinates, dense landmarks, and per-pixel masks.

However, DeepFashion2 images cannot be directly used for Virtual Try-On, which requires a frontal-view person with at least the upper body fully present and without large occlusion in relatively bright lighting conditions. Therefore, a two-stage data filtering process was employed for both the training and validation sets.

### A.1. Data Filtering Processes

At the first stage of filtering, we use DeepFashion2 [11]’s provided annotations to keep only the images with labels “frontal viewpoint”, “no zoom in” and “slight occlusion”. Besides, we filtered out the image sourced from customers in dark rooms, as shown in Fig. 10. After the initial filtering and we obtain a detailed data analysis for the data distribution. As shown in Fig. 12, the proposed Street TryOn benchmark contains a diverse set of garments in various categories.

Subsequently, in the second stage of filtering, the focus was on identifying images that portrayed the entire upper body of the models. We run the DensePose detection [13], which also detects human bounding boxes on these images. We discarded images without human bounding boxes detected and images with the person present horizontally (e.g., “has\_large\_occlusion\_torso”, “has\_watermark” and lying down) or images with bounding boxes in an aspect ratio larger than 5 : 8. We then pad the human bounding box

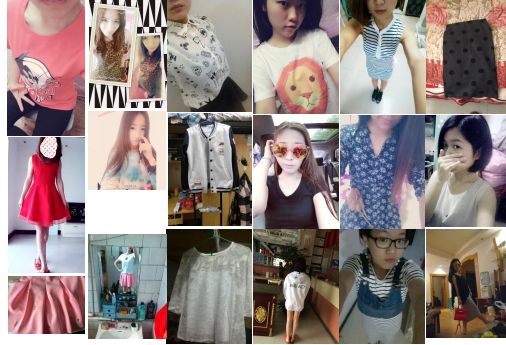


Figure 10. Example DeepFashion2 images that are not feasible for virtual try-on tasks and filtered out.

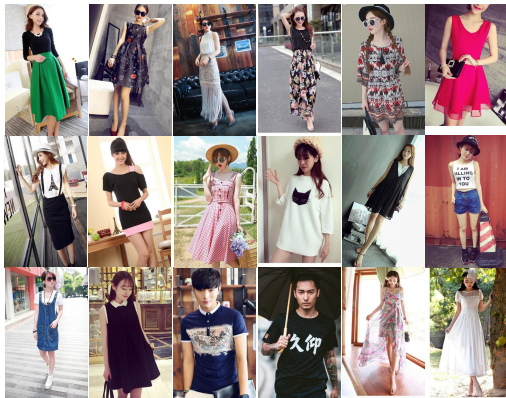


Figure 11. Examples of the selected DeepFashion2 images after cropping, which are included in the proposed Street TryOn Benchmark.

to make its aspect ratio 5 : 16, cropped the person from the images, and resized it to 512 × 320.

Following these two stages of meticulous filtering, the dataset was refined to encompass 12,364 images for the training set and 2,089 for the validation set. The examples of the selected and processed images can be found in Fig. 11.

### A.2. Data Statistics

Because each image in the DeepFashion2 dataset has rich annotation provided, we further investigate the annotations of the Street TryOn benchmark derived from DeepFashion2, and we obtain a detailed data analysis for the data distribution. As shown in Fig. 12, the proposed Street TryOn benchmark contains a diverse set of garments in various categories. Next, we looked into the images in the test set and manually labeled six attributes for each image, which are “is\_full\_body”, “is\_frontal\_view”, “has\_arm\_around\_torso”, “has\_large\_occlusion\_torso”, “has\_watermark” and “has\_padding”. These labels can be used to divide the validation set into different difficulty levels in the

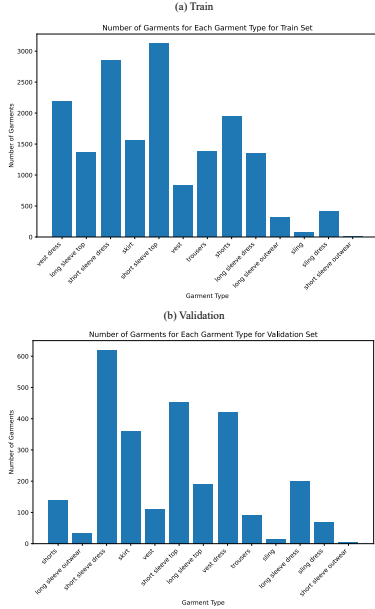


Figure 12. The number of garments in each garment type.

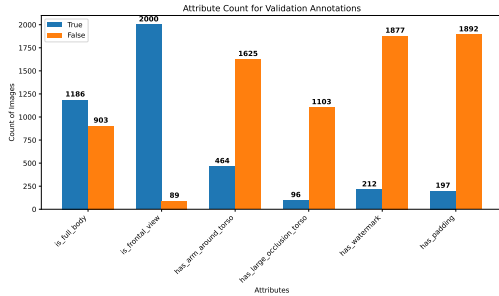


Figure 13. The distribution of manually labeled attributes in the test set.

future. The attribute distributions can be found in Fig. 13.

Since DeepFashion2 is a fashion retrieval dataset that originally contains multiple images for the same garments (by sharing the same ‘garment\_id’), we further investigate if we can build image pairs to enable paired training and validation for virtual try-on tasks. After the filtering processes, in the Street TryOn benchmark, there are 14% unique images without any other images labeled as the same garments. For the rest of the images, although the DeepFashion2 annotation suggests they have potentially paired images, the annotation is too noisy to be directly used to construct pairs, because the color variations of garments are not distinguished by the DeepFashion2’s garment\_ids, as shown in Fig. 14. Therefore, if one wants to build paired images for the Street TryOn benchmark in the future, additional manual annotation would be necessary.



Figure 14. The images that share the same ‘garment\_id’ in the DeepFashion2 Dataset. Color variations cannot be distinguished.

## B. DensePose Perturbation with Cosine Noise

As mentioned in the main paper, when we train the DensePose correction module, a cosine noise is added to the DensePose’s pixel values to mimic the imperfect DensePose alignment at the test time. This way, we can train it without paired data but still achieve robust performance at the test time.

Fig. 15(A) shows how the imperfect DensePose prediction causes warping distortion when we transform a garment from one pose to another. Clearly, in the visualized UV overlapping, the source DensePose and the target DensePose are not perfectly matched.

After observing the misalignment patterns, we propose to use a cosine perturbation to mimic this misalignment. Given a person’s DensePose  $P_H$ , in which each pixel  $(i, j)$  contains a  $(u, v)$  coordinate to map the person into UV space as  $P_H[i, j] = (u, v)$ , we add a cosine noise to its pixel values as

$$\tilde{P}_H[i, j] = \left( u + k_1 \cos(\alpha_1 u + \beta_1), v + k_2 \cos(\alpha_2 v + \beta_2) \right), \quad (5)$$

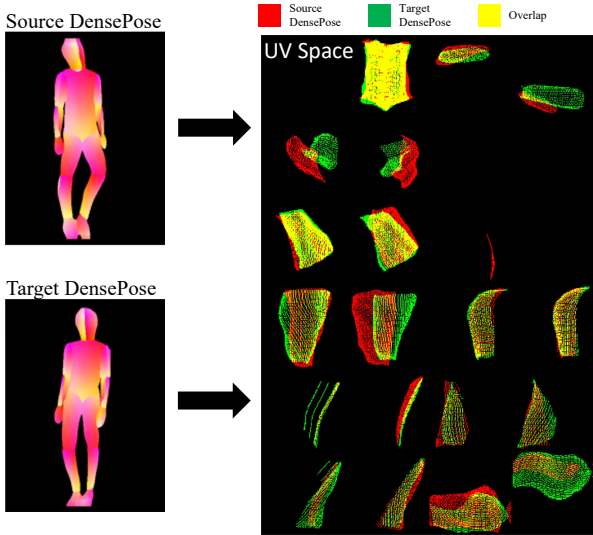
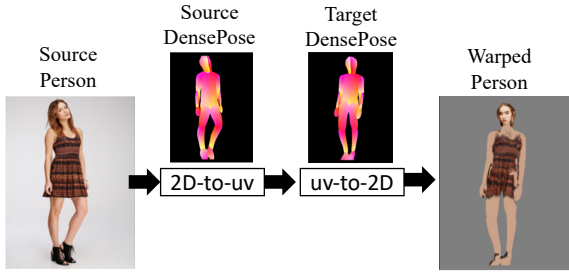
where  $k_1, k_2, \alpha_1, \alpha_2, \beta_1$  and  $\beta_2$  are randomly sampled coefficients for each UV map in DensePose  $P_H$ . As shown in Fig. 15(B), the cosine perturbation can effectively simulate the DensePose misalignment at the inference time. Therefore, with the cosine perturbation, we can mimic the inference scenarios during the training time without paired data.

## C. Additional Implementation Details

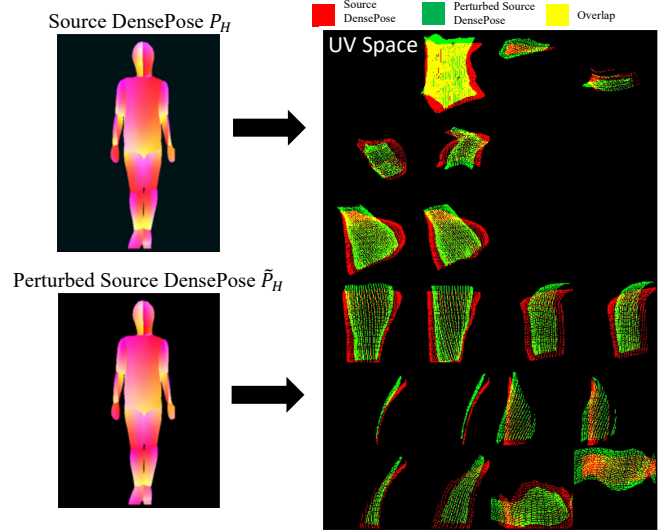
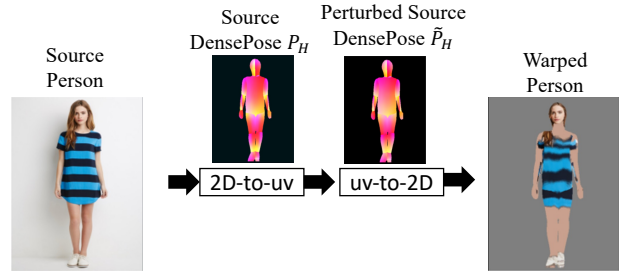
### C.1. Pre-trained Diffusion Models

Here, we provide additional implementation details of the diffusion models used in this work.

We set the inference steps for both the skin and refinement diffusion inpainters as 20. The guidance scale for both is 7.5. The skin inpainter has the negative prompt set as “art, clothes, garments, long-sleeves, sleeves, cloak, loose, thick clothes, loose clothes, pants, shirts, skirts, dresses, long jackets, jackets, cloth between legs, cloth around the body, cloth around arms.” The refinement diffusion inpainter uses a negative prompt as “blurry, cracks on skins, poor shirts, poor pants, strange holes, bad legs, missing legs, bad arms, missing arms, bad anatomy, poorly drawn face, bad face, fused face, cloned face, worst face, three crus, extra crus,



(A) DensePose Misalignment at the Inference Time



(B) Mimicked DensePose Misalignment at the Training Time

Figure 15. **DensePose Perturbation with Cosine Noise.** The example full-body person images are from the DeepFashion dataset [25] and are only used in this figure for illustration purposes. In this illustration, the full person is warped to demonstrate how the 24 UV maps in DensePose (for 24 different body parts) are misaligned. In the final warped image, we fill the skin with the average skin color for visualization.



Figure 16. The detected garment DensePose.

fused crus, worst feet, three feet, fused feet, fused thigh, three thighs, fused thigh, extra thigh, worst thigh, missing fingers, extra fingers, ugly fingers, long fingers, horn, extra eyes, huge eyes, 2girl, amputation, disconnected limbs, cartoon, cg, 3d, unreal, animate”.

As defined by the pretrained diffusion inpainter [9], at the inference time, it takes a concatenation of noise, the latent masked image, and the mask as the input to start de-

noising. Instead of directly using the Gaussian noise, our noise is built by first broadcasting the mean features into each segmentation class for the latent masked image based on the predicted tryon human parse  $M_T$  and adding noises to it with timestep as 999.

## C.2. Garment DensePose Detection

For preprocessing, we implement and train the garment DensePose Detection algorithm proposed in the prior work of Cui et al. [5] at resolution  $256 \times 192$ . Then, we resize the detected DensePose to the desired resolutions. The examples of detected garment DensePose can be found in Fig. 16.

## D. More Visual Results

In this section, more visual results are presented to verify the effectiveness of our approach.

### **D.1. Shop2Model Test**

More results can be found in the Shop2Model test on VITON-HD in Fig. 17 and Fig. 18, comparing with PFAFN [12], FS-VTON [17], SDAFN [2] and GP-VTON [35].

### **D.2. Street2Street Test**

We finally show more results for our Street2Street try-on with intermediate outputs in Fig. 19 and Fig. 20.

### **D.3. Ablation Study**

Here, we also provide more examples of ablation studies to validate the effectiveness of each component in the design of our approach in Fig. 21.



Person

Garment

PFAFN

FS-VTON

SDAFN

GP-VTON

Ours

Figure 17. More examples for Shop2Model test on VITON-HD benchmark [3] 1.





Person

Garment

PFAFN

FS-VTON

SDAFN

GP-VTON

Ours

Figure 18. More examples for Shop2Model test on VITON-HD benchmark [3] 2.



Figure 19. More examples for Street2Street test for top try-on.

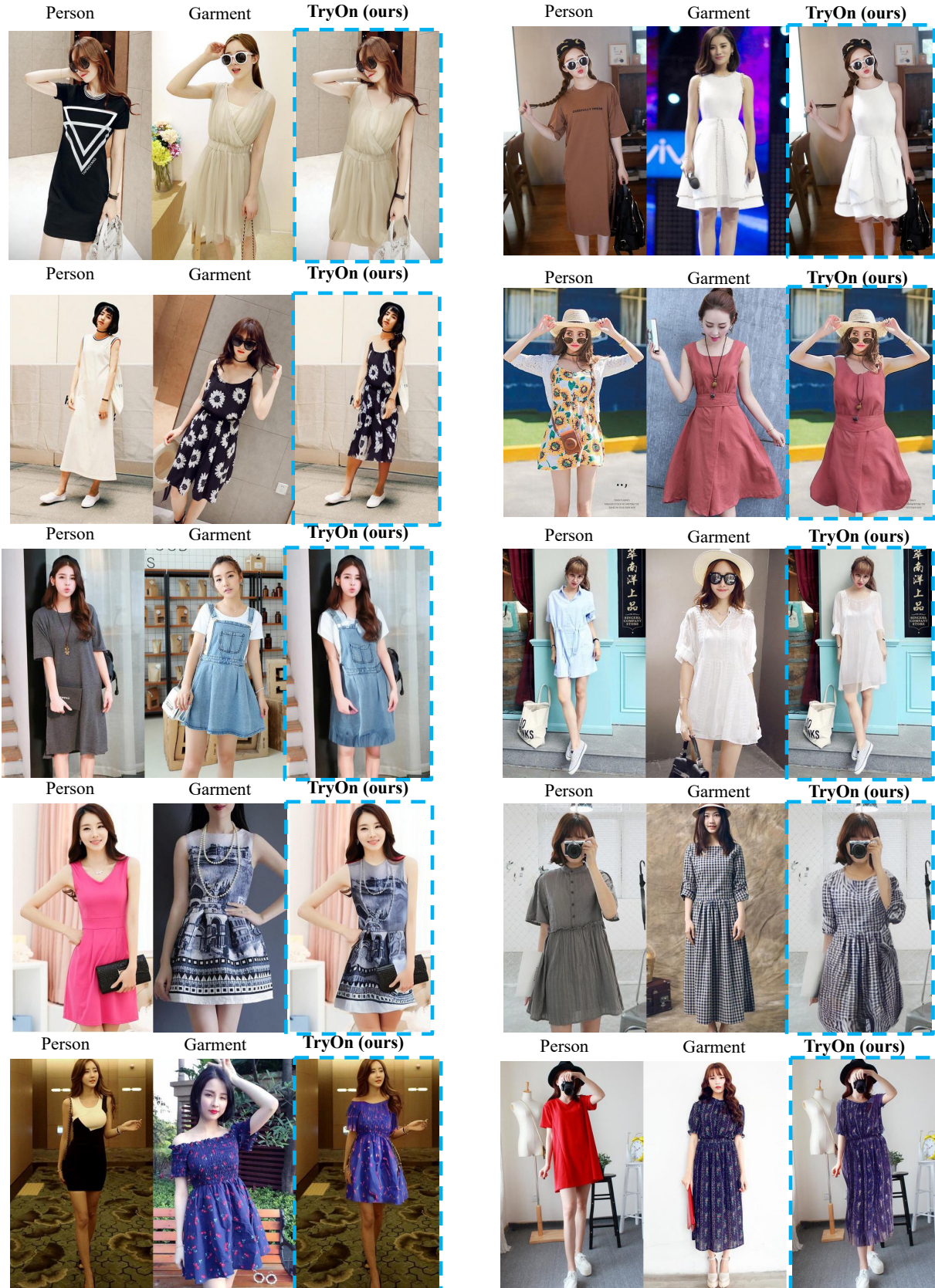


Figure 20. More examples for Street2Street test for dress try-on.

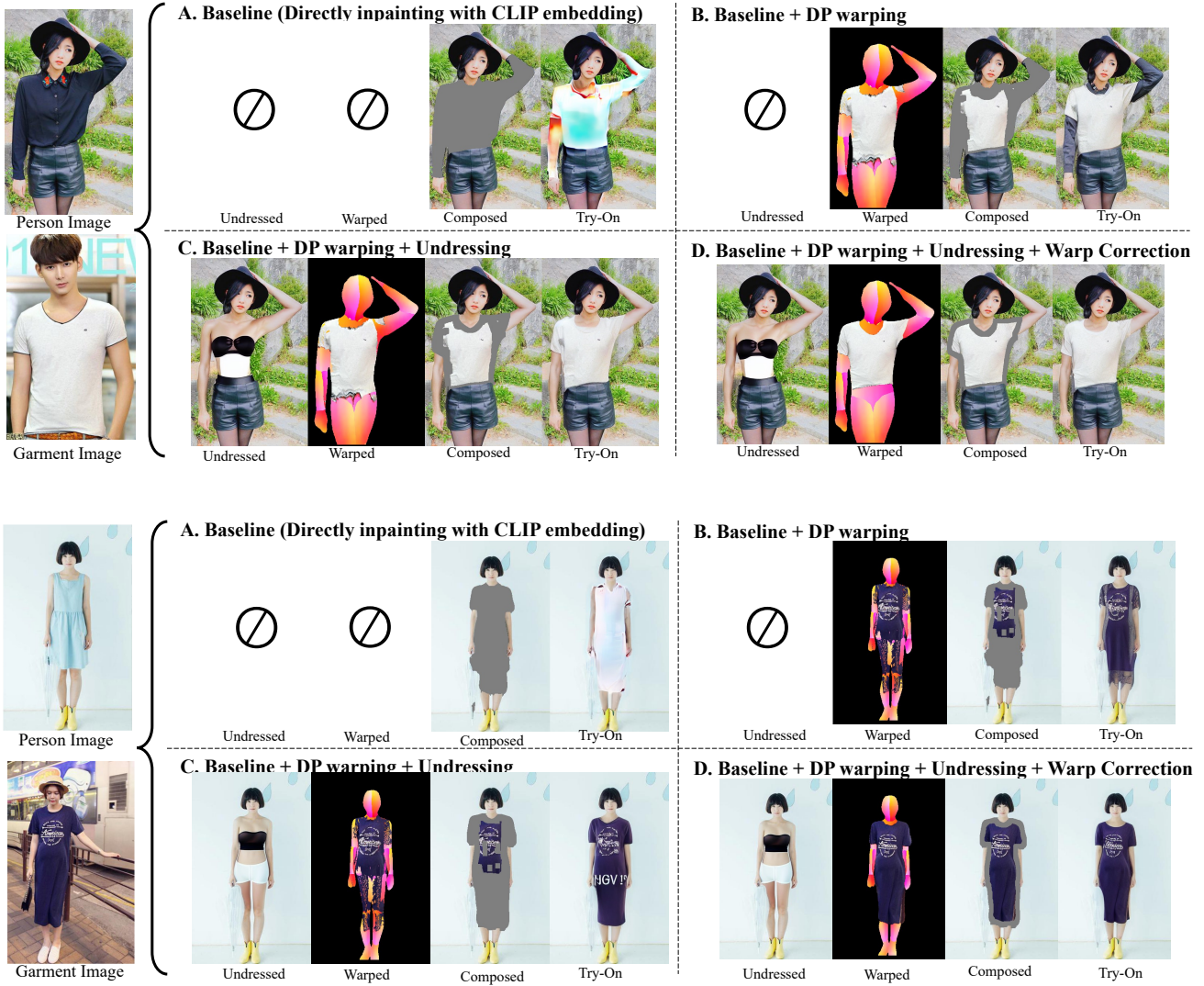


Figure 21. More examples for the ablation study to verify the effectiveness of each component in the proposed method.